Layout Considerations for 2D Planar Waveguide OXC with Integrated Lens Pair

Author/Contributor:
Kwok, Chee; Mackenzie, Mark; Peng, Gang-Ding

Publication details:
Proceedings of Photonics: Design, Technology & Packaging
pp. 215-222

Event details:
Photonics: Design, Technology & Packaging
Perth, Australia

Publication Date:
2003

Publisher DOI:
http://dx.doi.org/10.1117/12.523233

License:
https://creativecommons.org/licenses/by-nc-nd/3.0/au/
Link to license to see what you are allowed to do with this resource.

Downloaded from http://hdl.handle.net/1959.4/43064 in https://unsworks.unsw.edu.au on 2023-03-30

Layout considerations for 2D planar waveguide OXC with integrated lens pair

Mark Mackenzie, Chee Yee Kwok and G. D. Peng

The University of New South Wales

ABSTRACT

This paper reports on the scalability of MEMS optical cross-connect (OXC) switches which use 2D planar waveguide architecture and an integrated waveguide lens to enhance free space propagation. The optical loss, total device area and ease of integration with MEMS micromirrors are considered for three competing layout configurations.

Keywords: Collimating Lens, MOEM Switch, Graded Index

1. INTRODUCTION

The field of optical switching has generated considerable interest within the MEMS research community. This is hardly surprising as a MEMS solution to optical switching combines the advantages of optical switching (low insertion loss, low crosstalk, insensitivity to wavelength and polarisation, and scalability)[1] with the ability to significantly reduce overall device dimensions. In particular, MEMS can be applied to optical cross connects (OXCs) which are a critical component for the provision and restoration of optical networks.[2]

OXCs come in two types — 2D and 3D, depending on which dimensions the optical beams travel in. In the 2D $N \times N$ OXC the signals travel over an array of N^2 on/off micromirrors. The optical signals all travel in the two dimensional plane. In the 3D OXC the optical beams are 'steered' in three dimensions by using $2N$ gimbal mounted micromirrors.[3]

When considering an OXC which must be scaled to high port counts (greater than 32×32) a 3D device is clearly the best choice. This is because of the high insertion loss and large chip area required for the 2D device.[4] However, 2D OXCs based on planar waveguide technology does offer the unique advantage of being able to integrate the switching function with existing planar waveguide components such as the the AWG.[5]

When interfacing the optical circuit to the MEMS micromirror switches, collimation is required to allow the optical beam to propagate a reasonable distance in free-space. This can be achieved using lenses such as the graded index (GRIN) fibre lens[6] or the spherical lens.[7] In order to achieve collimation in planar waveguide circuits an integrated waveguide lens pair has been proposed.[8]

In this paper, the lens pair is considered in various modular switch layouts to find the most appropriate layout for use in a planar waveguide OXC.

2. INTEGRATED WAVEGUIDE LENS PAIR

The integrated waveguide lens pair is illustrated in Fig. 1. The lens pair allows free-space propagation of an optical signal between two opposing waveguides with minimal loss. Each lens consists of doped silica with a parabolically graded refractive index profile (essentially a slab GRIN lens) to focus light in the vertical direction. The lenses have a curved front-face to focus light in the horizontal direction.

The fabrication of the lens pair uses standard hollow cathode PECVD[9] and RIE techniques. This allows the fabrication of the lens pair to be integrated with the fabrication of other planar waveguide photonic devices.

Further author information:
Mark R. Mackenzie: E-mail: markm@unsw.edu.au, Telephone: 612 9385 5395
Chee Yee Kwok: E-mail: c.kwok@unsw.edu.au, Telephone: 612 9385 5300
G. D. Peng: E-mail: g.peng@unsw.edu.au, Telephone: 612 9385 4014
Address: School of EE&T, The University of New South Wales, Sydney 2052, Australia

Photonics: Design, Technology, and Packaging, edited by Chennupati Jagadish, Kent D. Choquette, Benjamin J. Eggleton, Brett D. Nener, Keith A. Nugent, Proc. of SPIE Vol. 5277 (SPIE, Bellingham, WA, 2004) · 0277-786X/04/$15 · doi: 10.1117/12.523233

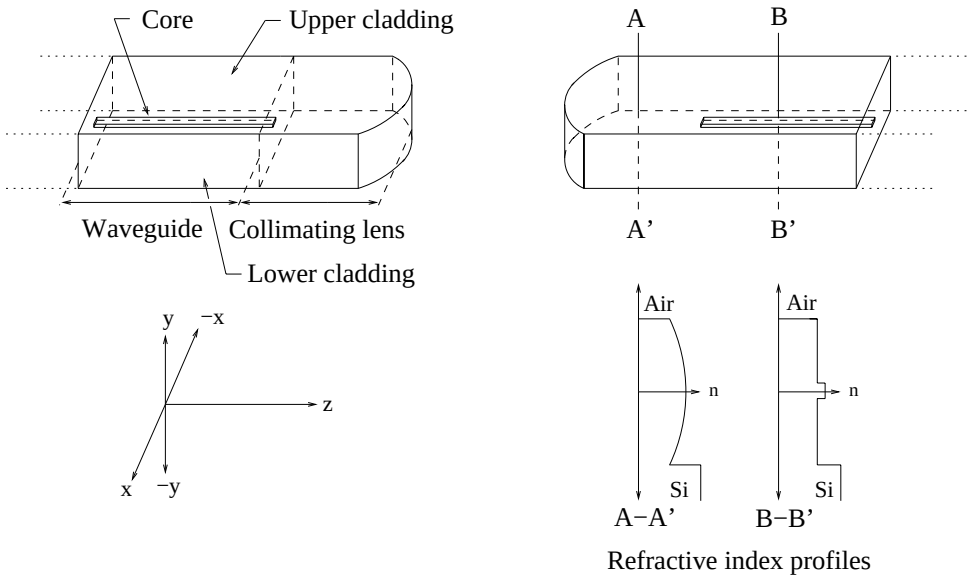

Figure 1. Integrated collimating waveguide lens pair.

The design of the lens pair has been described in detail previously.[8] The design process involves matching the spot size of the optical beam at various points as it propagates from the transmitting waveguide, through the lens pair and free-space to the receiving waveguide. The lens pair is designed for a particular propagation distance — the optical loss will be a minimum at this point.

For any one particular design length, a number of lens solutions are possible. The design is obtained by considering a number of trade-offs such as the lens length (which influences the horizontal spot size of the beam as it exits the lens), and the waveguide spot size.

Fig. 2 shows the calculated propagation loss (excluding the air/glass interface reflection loss) as a function of distance for three separate lens designs. The lenses are designed for free space propagation lengths of $100\mu m$, $200\mu m$ and $300\mu m$, and show minima at these distances. To allow comparison with the uncollimated case, the propagation loss for a Gaussian beam with spot-size of $\omega = 4.0\mu m$ is also shown.

3. FREE-SPACE OPTICAL SPOT-SIZE

The role of the focussing lenses is essentially to take the small optical spot size of the guided light (be it a planar waveguide or optical fibre) and increase the spot-size so that it can propagate in free-space without significant divergence. However, as the spot size is increased the micro-mirrors must be aligned to an increasingly tight angular tolerance.[10]

The trade-offs between available propagation distance and angular alignment tolerance is illustrated in Fig. 3. For each initial spot size ω_o the propagation distance is found (solid line) which would cause 0.5 dB loss. The mirror angular misalignment which would cause loss of an additional 0.5 dB at this distance and spot size is then also found (dashed line).

4. PLANAR WAVEGUIDE LAYOUT CONFIGURATIONS

Three competing 2D planar waveguide OXC architectures have been analysed to determine the most suitable switch layout. Two of the architectures use the integrated waveguide lens to minimise the free-space propagation loss. The following points were considered as each OXC architecture is scaled to higher port counts:

- optical loss over the range of switching paths,

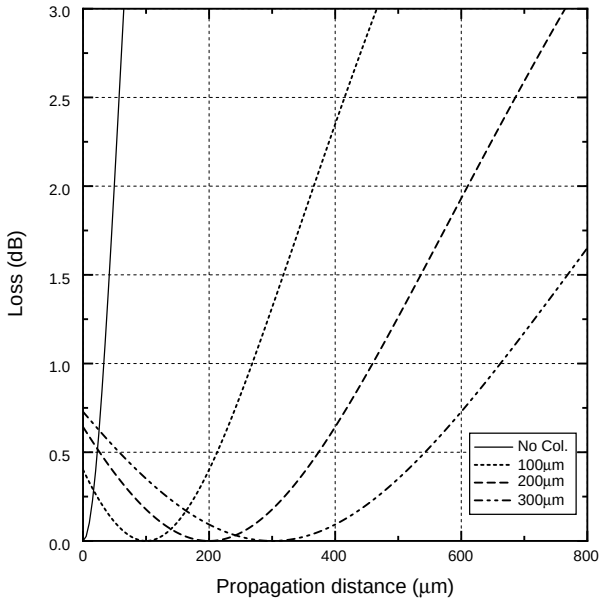

Figure 2. Estimated optical loss of the collimated beam with ideal propagation lengths of $100\mu m$, $200\mu m$ and $300\mu m$ (does not include air/glass interface loss). The loss of an uncollimated beam with spot-size $\omega = 4.0\mu m$ is shown for comparison.

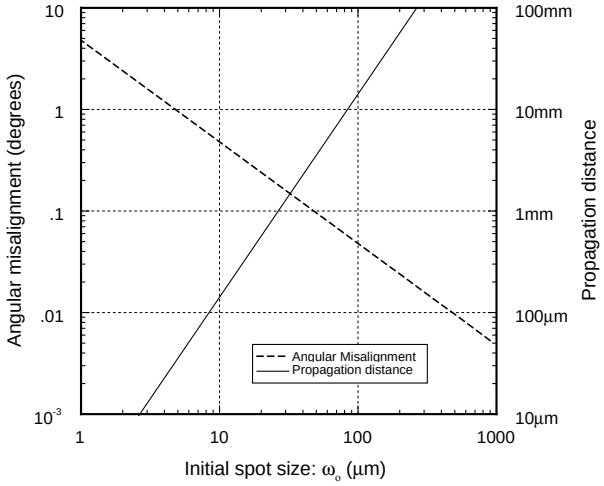

Figure 3. Propagation distance causing optical loss of 0.5 dB as a function of spot-size (solid line) and and mirror angular misalignment θ_m which would cause an additional loss of 0.5 dB at this distance (dashed line).

- tolerence to mirror angular misaligment, and
- total OXC area.

4.1. The uncollimated waveguide OXC design

The uncollimated waveguide OXC architecture is illustrated in Fig. 4. This architecture does not require collimation because the small free-space inter-waveguide gap does not cause excessive optical loss.

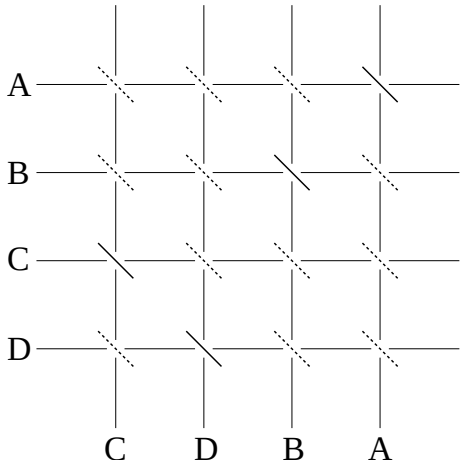

Figure 4. Uncollimated waveguide OXC.

An OXC of this type has been fabricated previously.[11] The authors expected a propagation loss of 0.5 dB per free-space gap[11] and a waveguide loss of 0.4 dB cm^{-1}.[12] The micro-mirrors were actuated by a novel bistable comb drive actuator. Each actuator occupied an area of approximately 1.56 mm^2.

4.2. The 2×2 modular OXC

Fig. 5 shows a 4×4 OXC comprised from four 2×2 switching modules. The two by two switching module consists of four pairs of single mode planar waveguides, each terminated with an integrated waveguide lens. The intervening space contains a matrix of four switching mirrors. Opposing lenses are separated by the 'ideal' free space propagation length.

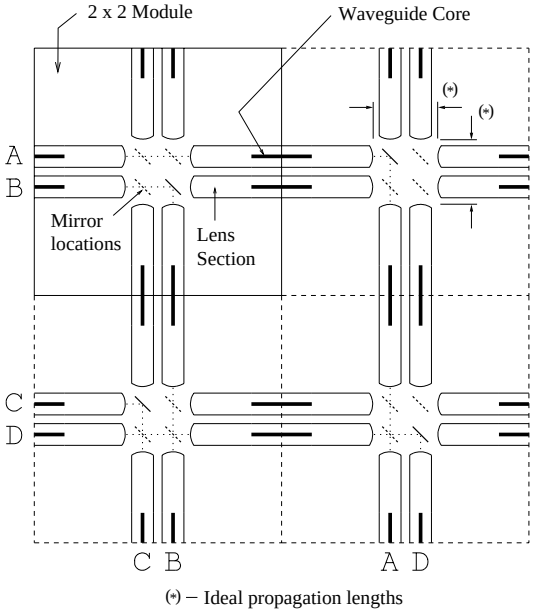

Figure 5. Four 2×2 switching modules cascaded to form a 4×4 OXC. The area of each module is approximately $2mm^2$.

When the optical signal is switched in one of the 2×2 switching modules, a higher loss penalty will be incurred because the free space propagation length differs from the optimal design value. The additional loss

incurred can be estimated from Fig. 2. However, within the higher port count device it is only necessary to switch at this non-optimal propagation length in *one* of the switching modules. All other free space propagation lengths will be at the optimal design value.

One disadvantage of the 2×2 modular OXC is that neighbouring micromirror actuators tend to interfere. Cantilevered micromirrors[13] are required, with the fixed ends of the cantilever at two opposite corners of the module. This increases the area taken by each module considerably.

To allow comparison with the other OXC layouts, a lens pair design with an optimal free-space propagation length of $200\mu m$ is considered. After allowing space for a cantilevered micromirror, the area of each 2×2 module is approximately 2mm^2.

4.3. The 4×1 modular layout

Fig. 6 shows a 4×4 OXC built by cascading four 4×1 switching modules. The lens pairs are arranged so that each free-space propagation length is at the optimal design length, regardless of the path taken by the optical beam.

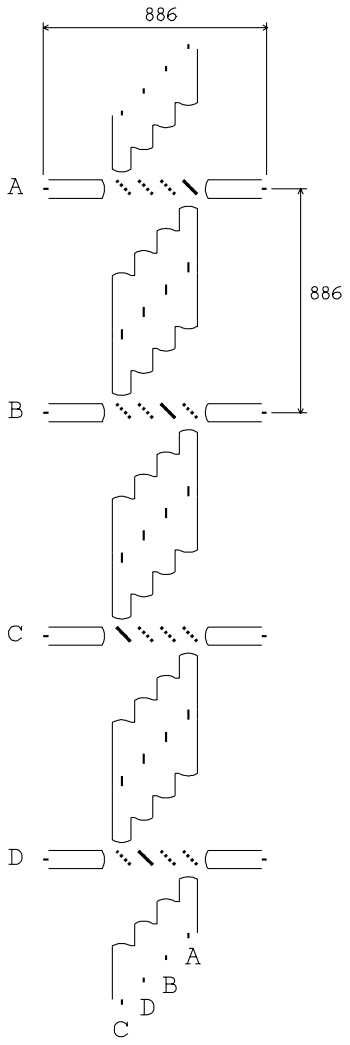

Figure 6. Four 4×1 switching modules cascaded to form a 4×4 OXC. The area of each module is approximately 0.8mm^2.

The 4×1 modular layout lends itself to integration with a micromirror array far more easily than the 2×2 layout. The micromirrors can be beam actuated[14,15] (fixed at two ends) and placed in a linear fashion without interfering with neighbouring micromirrors. This leads to a higher switching density.

For comparison purposes, a lens pair design with an optimal free-space propagation length of $400\mu m$ is considered. The area of each 4×1 module is approximately 0.8mm^2.

5. SUMMARY OF LAYOUT COMPARISON

Fig. 7 compares each component of the total insertion loss, and the estimated chip area for each of the three OXC architectures. The reflection loss at each air/silica interface is assumed to be 0.15 dB. The waveguide loss is assumed to be 0.04 dBmm^{-1}. There will inevitably be some fabrication error when producing the lens pairs.[8] The target loss for this error is 0.5 dB. The area taken by each module is indicated in sections 4.1, 4.2 and 4.3. The tolerance of each architecture to angular misalignment is gauged by calculating the mirror misalignment[10] which would cause an additional 1 dB propagation loss.

The resulting loss versus port count is shown in Fig. 8 (assuming no angular misalignment), and the estimated chip area is shown in Fig. 9.

	Waveguide only OXC (Fig. 4)	2×2 mod OXC (Fig. 5)	4×1 mod OXC (Fig. 6)
Reflection loss (dB)	$2 \times 0.15^a \times (2N-1)$	$2 \times 0.15 \times (N-1)$	$2 \times 0.15 \times (N+m-1)$ [b]
Waveguide loss (dB)	$0.04\text{mm}^{-1} \times 1.2\text{mm} \times (2N-1)$	$.04\text{mm}^{-1} \times 0.55\text{mm} \times (N-1)$	$.04\text{mm}^{-1} \times 0.04\text{mm} \times (N+m-1)$
Free-space loss (dB)	$0.5 \times (2N-1)$	0.22^c	0^d
Lens fabrication loss	NA	$FEL^e \times (N-1)$	$FEL \times (N+m-1)$
Alignment tolerance[f]	1.6°	0.29°	0.26°
Switch area (mm^2)	$N \times N \times 1.56$	$\frac{N}{2} \times \frac{N}{2} \times 2.0$	$N \times m \times 0.8$

[a] Loss caused by one air/glass interface.
[b] m =number of modules required horizontally=round$\uparrow\left(\frac{N}{4}\right)$
[c] Each signal switched once at 1.5 × non-optimal propagation length.
[d] All propagation lengths at optimal design value.
[e] Loss caused by lens fabrication errors such as offset or mask misalignment. Target value: 0.5 dB.
[f] Mirror angular misalignment which causes additional 1 dB loss.

Figure 7. Comparison of OXC architectures.

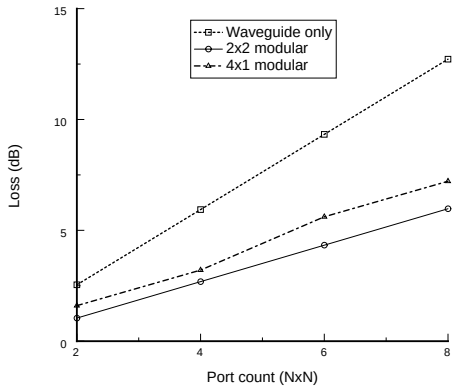

Figure 8. Loss vs port count.

As can be seen, the 2×2 and 4×1 modular OXCs have similar loss penalties when scaled to higher port counts. Actuator layout and the switch area density then become the dominating factors. As indicated in section

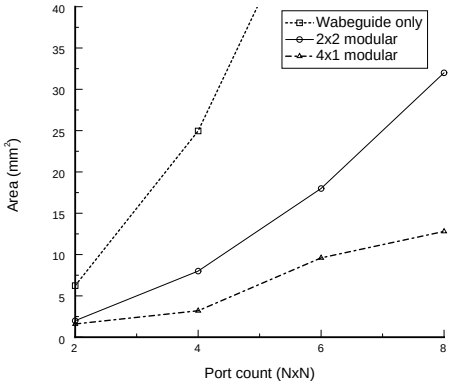

Figure 9. Chip area vs port count.

4.3, the 4×1 module lends itself more easily to integration with the micromirror array chip and so would be the most suitable planar waveguide OXC layout.

6. CONCLUSION

Three different layout architectures for planar waveguide MEMS OXCs have been considered. The most practical layout design for the planar waveguide OXC uses the 4×1 modular layout. This layout uses the least area, and has relatively good loss vs scalability characteristics. It is also the most suitable architecture for integration with MEMS micro-mirrors.

REFERENCES

1. R. A. Syms, "Scaling laws for mems mirror-rotation optical cross connect switches," *IEEE Journal of Lightwave Technology* **20**(7), pp. 1084–1094, 2002.
2. P. B. Chu, S. Lee, and S. Park, "Mems: The path to large optical crossconnects," *IEEE Communications Magazine* , pp. 80–87, March 2002.
3. V. A. Aksyuk, F. Pardo, C. A. Bolle, S. C. Arney, C. R. Giles, and D. J. Bishop, "Lucent microstar micromirror array technology for large optical cross connects," in *Proceedings of SPIE*, **4178**, pp. 320–324, 2000.
4. L. Lin and E. L. Goldstein, "Opportunities and challenges for mems in lightwave communications," *IEEE Journal of Selected Topics in Quantum Electronics* **8**(1), pp. 163–172, 2002.
5. M. Katayama, T. Kanie, H. Okuyama, T. Sano, K. Koyama, T. Sasaki, C. Hirose, T. Hattori, M. Nishimura, and S. Semura, "Micromachined curling optical switch array for plc-based integrated programmable add/drop multiplexer," in *OFC2001*, pp. WX4: 1–3.
6. L. Lin, E. L. Goldstein, and R. W. Tkach, "Free-space micromachined optical switches for optical networking," *IEEE Journal of Selected Topics in Quantum Electronics* **5**, pp. 4–9, 1999.
7. H. Toshiyoshi and H. Fujita, "Electrostatic micro torsion mirrors for an optical switch matrix," *Journal of Microelectromechanical Systems* **5**, pp. 231–237, 1996.
8. M. R. Mackenzie and C. Y. Kwok, "Theoretical analysis of integrated collimating waveguide lens," *IEEE Journal of Lightwave Technology* **21**(4), pp. 1046–1052, 2003.
9. M. V. Bazylenko, M. Gross, A. Simonian, and P. L. Chu, "Pure and flourine-doped silica films deposited in a hollow cathode reactor for integrated optic applications," *Journal of Vacuum Science Technology A* **14**(2), pp. 336–345, 1996.
10. L. Lin, E. L. Goldstein, and R. W. Tkach, "On the expandability of free-space micromachined optical cross connects," *IEEE Journal of Lightwave Technology* **18**, pp. 482–489, 2000.

11. L. Dellmann, W. Noell, C. Marxer, K. Weible, M. Hoffmann, and N. F. de Rooij, "4x4 matrix switch based on mems switches and integrated waveguides," *The 11th International Conference on Solid-State Sensors and Actuators Munich Germany* , pp. 1332–1335, 2001.
12. M. Hoffmann, P. Kopka, and E. Voges, "Low-loss fiber-matched low-temperature pecvd waveguides with small-core dimensions for optical communications systems," *IEEE Photonics Technology Letters* **9**(9), pp. 1238–1240, 1997.
13. P. Helin, M. Mita, T. Bourouina, G. Reyne, and H. Fujita, "Self-aligned micromachining process for large-scale, free-space optical cross-connects," *IEEE Journal of Lightwave Technology* **18**(12), pp. 1785–1791, 2000.
14. K. Yu, A. Michael, and C. Y. Kwok, "Novel bistable thermally actuated snap-through actuator for out of plane deflection," in *Device and Process Technologies for Microelectronics, MEMS, and Photonics*, SPIE, 2003.
15. A. Michael, K. Yu, and C. Y. Kwok, "Initially buckled, thermally actuated, and snapping bimorph microbridge," in *Device and Process Technologies for Microelectronics, MEMS, and Photonics*, SPIE, 2003.